ANALYTICAL MODEL FOR FLUID TEMPERATURE CHANGE DURING EXPANSION IN THE RESERVOIR

A Thesis

by

RAKA ISLAM

Submitted to the Office of Graduate and Professional Studies of
Texas A&M University
in partial fulfillment of the requirements for the degree of

MASTER OF SCIENCE

Chair of Committee,	A. Rashid Hasan
Committee Members,	Hadi Nasrabadi
	M. Sam Mannan
Head of Department,	A. Daniel Hill

May 2017

Major Subject: Petroleum Engineering

ABSTRACT

This research presents an analytical 1D radial-flow model for estimating the transient flowing-fluid temperature in a single-phase oil reservoir. The model allows fluid density, viscosity, and the J-T coefficient to vary with pressure and temperature. A rigorous thermodynamic expression based on fluid PVT behavior underpins the proposed model. The usual assumption of isothermal flow may be unsuitable in low-conductivity formations where large drawdowns occur. The increase in fluid temperature associated with Joule-Thompson (J-T) heating triggers the consequent changes in oil viscosity and density. This model is also extended to estimate flowing fluid temperature for single-phase gas. In case of gas, Joule-Thomson cooling is observed. The Joule-Thomson coefficient for a low pressure gas is usually positive and so it results in a temperature reduction as pressure decreases.

A detailed sensitivity analysis has shown the effect of production rate on reservoir heating and consequent changes in fluid properties. Specifically, we observed that fluid temperature increase above the original formation temperature occurs with a decrease in formation permeability, an increase in oil viscosity, and a decrease in overall heat-transfer coefficient. Of course, J-T heating increases with increasing flow rate.

Changes in reservoir temperature occur within about 100 ft from the wellbore assuming 1D radial flow. Overall, the lessons learned from this study illuminates the need for reevaluating tubular design, flow-assurance issues related to dissolved solids, and assessment of well productivity index arising from J-T heating.

We coupled a wellbore temperature model with our reservoir model to get a complete picture of temperature during production. Results from reservoir model (bottomhole pressure and temperature) are used in the wellbore model as inputs. The model is then validated with field data. Coupled reservoir/wellbore model is useful for analysis of flowing fluid temperature of whole production system.

DEDICATION

To Jasmine Jubery & Waqar Mohiuddin,

For all the laughter and love

ACKNOWLEDGEMENTS

I would first like to thank my thesis advisor, Dr A. Rashid Hasan, for his constant support and technical guidance. I am gratefully indebted to him for always steering me in the right direction whenever I ran into a trouble spot and for giving me time from his packed schedule every time I needed it. I would also like to thank Dr Sam Mannan and Dr Hadi Nasrabadi for serving as my committee member. I greatly appreciate their support and recommendations.

I would like to take this opportunity to thank Shah Kabir from C.S. Kabir Consulting, for his valuable insight and guidance.

I would like to express my gratitude to Dr Ibere Alves for giving me the opportunity to work as his Teaching Assistant.

Finally, thanks to my parents for believing in me, allowing me to pursue my dream without any interruption and for their patience and love & to my friends, for their continuous encouragement.

CONTRIBUTORS AND FUNDING SOURCES

Contributors

Part 1, faculty committee recognition

This work was supervised by a thesis committee consisting of Professor A. Rashid Hasan and Professor Hadi Nasrabadi of the Department of Petroleum Engineering and Professor Sam Mannan of Department of Chemical Engineering

Part 2, student/collaborator contributions

All work for the thesis was completed independently by the student.

Funding Sources

There are no outside funding contributions to acknowledge related to the research and compilation of this document.

NOMENCLATURE

A	=	cross sectional area, ft^2, L^2
B_o	=	oil formation volume factor, bbl/STB
B_{ob}	=	oil formation volume factor at bubble point, bbl/STB
c_t	=	total compressibility, 1/psi, Lt^2/m
c_p	=	system specific heat capacity, Btu/lbm.°F, L^2/t^2T
C_J	=	Joule-Thompson coefficient, °F/psi, TLt^2/m
h	=	formation thickness, ft, L
h_c	=	heat transfer coefficient, Btu/hr.ft^2.°F, $m/t^3/T$
H	=	enthalpy, BTU/lbm or lbm.ft^2/hr^2, mL^2/t^2
k	=	reservoir permeability, md, L^2
L_R	=	Relaxation parameter
M_A	=	Apparent Molecular Weight
p	=	pressure, psi, m/Lt^2
Δp_s	=	pressure drop due to skin, psi, m/Lt^2
P_e	=	Peclet number (= ur/α), dimensionless
$\dot{Q}$	=	net heat transfer rate between the system and surroundings, Btu/hr/ ft^2, m/Lt^3
q	=	volumetric flow rate, ft^3/hr, L^3/t
r	=	radius, ft, L
r_e	=	external reservoir radius, ft, L

r_w	=	wellbore radius, ft, L
R	=	gas constant
Rs	=	solution gas oil ratio, RB/STB
S	=	saturatuion
S_o	=	oil saturation
S_w	=	water saturation
t	=	time, hr, t
T	=	fluid temperature, °F, T
T_e	=	fluid temperature at reservoir external boundary, °F, T
T_{ei}	=	undisturbed earth or formation temperature, °F, T
T_i	=	initial reservoir temperature, °F, T
u	=	velocity, ft/hr, L/t
$\vec{u}$	=	superficial velocity, ft/hr, L/t
U	=	fluid internal energy, lbm.ft^2/hr^2, mL^2/t^2
V	=	Fluid expansivity, ft3/lbm, L^3/m
Z	=	gas compressibility factor
λ	=	reservoir thermal conductivity, Btu/hr.ft.°F, TLt^2/m
α	=	thermal diffusivity (= $\lambda/\rho c_p$), ft^2/hr, L^2/t
β	=	Volume expansivity, ^{o}F^{-1}
γ_o	=	oil gravity, ^{o}API
γ_g	=	gas gravity (air=1), dimensionless
ρ	=	density, lbm/ft^3, m/L^3

ρ_o	=	oil density, lbm/ft^3, m/L^3
ρ_w	=	water density, lbm/ft^3, m/L^3
ρ_f	=	formation density, lbm/ft^3, m/L^3
σ_o	=	Joule Thomson throttling coefficient of oil = C_J/ρ,
σ_w	=	J-T throttling coefficient of water, Btu/lbm-psi/L^3/m
ϕ	=	porosity
μ	=	viscosity, cp
μ_{oD}	=	dead oil viscosity, cp
μ_o	=	unsaturated oil viscosity, cp

TABLE OF CONTENTS

Page

LIST OF FIGURES

Page

LIST OF TABLES

Page

CHAPTER I

INTRODUCTION

1.1 Introduction and Literature Review

The assumption of isothermal reservoir temperature is the norm in most engineering calculations. As fluid flows from the reservoir toward the wellbore under large drawdowns, the Joule-Thompson (J-T) effect may play a large role in influencing the fluid temperature. Changes in oil temperature affect its viscosity, density, and other properties. These properties, in turn, influence pressure gradient, and the J-T coefficient. This study attempts to understand the sensitivity of J-T heating on various properties of reservoir fluid and their interdependence.

Lauwerier (1955) developed a mathematical model for temperature distribution in oil reservoir. He studied a case in which heat is supplied by hot fluid injection where the flow pattern is linear. Thermal conductivity is assumed zero in the direction of the flow. No Joule-Thompson effect was taken into consideration.

The results of various analytical temperature models (Avdomin, 1964, Lauwerier, 1955) were studies by Spillette (1965). He provided a numerical solution and validated it with the previous models.

Typical reservoirs that are worthy of flow condition of interest include those in deep, tight, and overpressure systems. To understand flow behavior in this type of environment, App (2009, 2010) did the pioneering study by developing a nonisothermal reservoir simulator for single-phase oil flow by coupling mass, and energy-balance equations with Darcy's law. This numerical model incorporates the principal heat-transfer

mechanisms in the reservoir, including heat transfer from the reservoir to over and under-burden formations. Most notably this model can evaluate changes in well productivity due to J-T heating in high-pressure, high-drawdown reservoirs arising from fluid viscosity decrease with temperature.

Ramazanov and Nagimov (2007) proposed an analytical model for single phase oil and non-steady state flow. Heat transfer mechanism in their model included convection and heat transfer due to fluid expansion. Radial conduction is presumed to be insignificant. Subsequently, Ramazanov et al. (2013) proposed a similar numerical model in which they showed that the impact of radial conduction to the fluid-temperature distribution in a reservoir is minimal during constant-rate production. Their results with and without radial conduction indicated that the effect of radial conduction to fluid temperature distribution is negligible at constant production rate.

Duru and Horne (2010) incorporated Joule-Thomson heating and cooling in a model. Heat transfer by conduction and convection was also taken into account. Operator Splitting and Time Stepping technique (OSATS) was applied in their model in order to solve the problem at hand. Coupled with wellbore model by Izgec at al (2007), the principal objective of the study was to provide improved estimation of reservoir properties through a complete production system.

In a more recent analytical model for steady-state flow, App and Yoshikawa (2013) showed that the fluid temperature changes with producing rate, reservoir permeability, and drawdown, among other variables. They showed that the Peclet number ($Pe = ur/\alpha$) implicitly handles permeability through fluid velocity. This dimensionless

parameter helps to gauge changes in fluid temperature at various flow conditions in diverse rock, fluid, and thermal properties.

Joule-Thomson effect for low pressure gas has been studied by App (2009). Low pressure gas production in a 1-D radial thermal simulator was carried out to show the effect of temperature reduction. To demonstrate the isothermal nature, the values from a drill stem test is is presented and modeled.

The analytical frame also became the cornerstone for the development of a 1D radial model proposed by Chevarunotai et al. (2015), which included heat transfer to or from over and under-burden formations. This simplified modeling approach essentially reproduced the results of App's (2010) numerical model. Based on calculations of Peclet numbers, they also found that ignoring conductive heat transport appears reasonable for field production rates of interest.

1.2 Problem Statement

In the last decade, more and more developments have been carried out in the area of challenging reservoirs like tight oil and gas, deep water assets etc. Whenever large pressure drawdown is involved, it becomes imperative to take into account Joule-Thompson phenomena. As a result, the insertion of J-T phenomena is important in the prediction of flowing fluid temperature.

If we can estimate the flowing fluid temperature more accurately, it helps us to predict fluid properties like viscosity, density etc. Especially in near wellbore region, where temperature and pressure change is more significant, the changes in fluid properties

becomes vital in calculation of fluid temperature. Temperature assessment in turn helps us to get a more accurate well productivity estimation. A robust analytical solution allows us accurate calculation keeping computational cost nominal.

Analytical reservoir temperature model, when coupled with wellbore model, gives us temperature profile at the wellbore. A lot of different completion design requires wellbore temperature profile. It is valuable for drilling calculations too. By doing inverse calculation, it is possible to find out reservoir permeability and other reservoir properties from temperature calculation.

1.3 Research Objectives

This research extends the earlier study of Chevarunotai et al. (2015) by incorporating the variation of fluid properties of density, viscosity, and the J-T coefficient. Specifically, we have developed a robust expression for estimating a fluid's J-T coefficient from its PVT relationships. This analytical model is useful in estimating the flowing-fluid temperature during the flow of single-phase oil in a reservoir. In particular, when large drawdowns are associated with moderate production rates (> 5,000 STB/D) in relatively low-permeability reservoirs (< 20 md), a significant rise in oil temperature (> 20 ^{o}F) may occur due to the J-T effect with the expansion of compressible oil.

We extended our model for gas as well. By incorporating gas properties in the temperature model, we calculated the temperature distribution for flowing gas at different initial pressure. Depending upon the pressure range, Joule-Thomson effect can result in either a heating or cooling effect for gas.

Analytical reservoir temperature model is coupled with a wellbore temperature model for getting temperature profile for complete production system. Pressure and temperature profile for bottomhole and wellhead can be useful for many calculations during completion and drilling.

Sensitivity analysis of this study offers an improved understanding of reservoir types and fluid environments where Joule-Thomson effect shows a critical role in reservoir flowing fluid temperature and eventually affects the productivity of the well.

CHAPTER II

MODEL DEVELOPMENT

2.1 Analytical Model

Our analytical model for transient flowing-fluid temperature is based on the work initiated by Chevarunotai et al, (2015). The reservoir model, schematically shown in Fig. 1, represents the 1D radial flow of single-phase oil at a constant rate. The well is assumed to be in the middle of the reservoir. We also assume that reservoir porosity and permeability remains unchanged and fluid temperature and pressure at the reservoir boundary remains constant (that is, dp/dt = 0). In addition, for the purpose of solving the differential equation, changes in fluid properties are assumed to be negligible. These assumptions led to the following expression for oil temperature as a function of radial distance and time:

$$T(r,t) = T_i + \frac{C}{2B} e^{\frac{H(Ar^2+2Bt)}{2B}} Ei\left[-\frac{H\left(Ar^2+2Bt\right)}{2B}\right] - \frac{C}{2B} e^{\frac{HAr^2}{2B}} Ei\left[-\frac{HAr^2}{2B}\right] \quad (2.1)$$

In deriving Eq. 1, radial heat conduction was neglected, an assumption that appears very robust for deep water assets where flow rates predominate (Chevarunotai et al 2015). Appendix A presents the parameters A through H in Eq. 2.1.

2.2 Energy Balance in the Reservoir

The general form for thermal energy balance used in deriving Eq. 2.1 is given below:

$$\frac{\partial}{\partial t}\rho\widehat{U} = -\left(\nabla\cdot\rho\widehat{U}\vec{u}\right) - (\nabla\cdot\vec{q}) - p(\nabla\cdot\vec{u}) - (\vec{\tau}:\nabla\vec{u}) + \dot{Q} \quad (2.2)$$

Here $\widehat{U}$ is fluid internal energy, ρ is fluid and/or rock density, and $\vec{u}$ is fluid local velocity. The $\nabla \cdot$ term generally represents net input rate of energy per unit volume of the system.

The comprehensive energy balance equation for the system, after writing enthalpy in term of pressure and temperature for each component:

$$\left[\emptyset s_o \rho_o c_{po} + \emptyset s_w \rho_w c_{pw} + (1-\emptyset)\rho_f c_{pf}\right]\frac{\partial T}{\partial t} + \rho_o u_r c_{po}\frac{\partial T}{\partial r} + \rho_o u_r \sigma_o \frac{\partial p}{\partial r} +$$

$$\left[\emptyset s_o \rho_o \sigma_o + \emptyset s_w \rho_w \sigma_w - 1\right]\frac{\partial p}{\partial t} = \frac{1}{r}\frac{\partial}{\partial r}\left[\lambda r \frac{\partial T}{\partial r}\right] + \dot{Q} \qquad (2.3)$$

The first two terms of Eq 2.3 are energy change due to temperature transient and convective heat transfer. The third term represents Joule-Thomson effect and the fourth term is energy change due to pressure transient state. The first term on the right hand side of Eq. 2.3 represents energy change from radial heat conduction and $\dot{Q}$ represents heat transfer to or from over and under-burden formation.

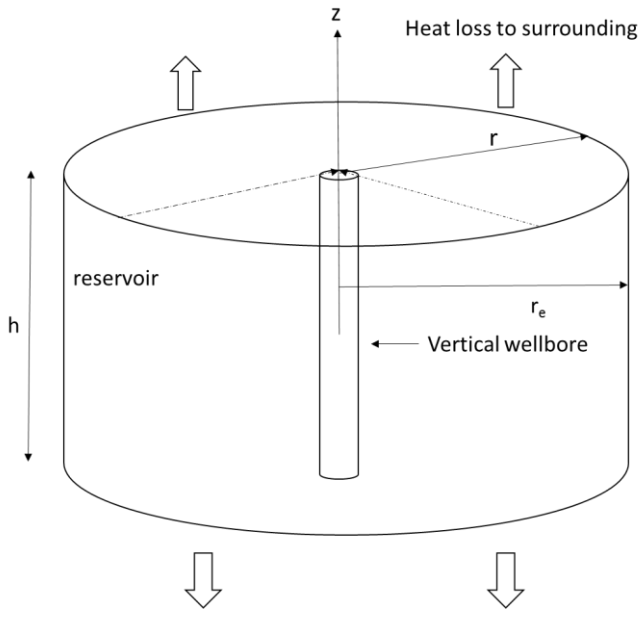

Fig. 1: Schematic of reservoir-wellbore model.

Note that Eq. 2.1 was developed assuming fluid property variation to be negligible. However, to demonstrate the effect of fluid properties and other parameters, temperature computation with Eq. 2.1 involved variation of fluid properties with pressure and temperature. This apparent contradiction still leads to reasonable solutions as will be shown later. Computation of fluid properties with variable pressure and temperature require appropriate expressions. Appendix B presents correlations for oil viscosity and density in terms of pressure and temperature. A rigorous thermodynamic expression for J-T coefficient computation, based on fluid PVT behavior, is also presented in Appendix B.

2.2 Reservoir Analytical Inflow Model

Analytical reservoir inflow models for single-phase constant rate production has been incorporated in this study for bottomhole pressure and temperature calculation. We can also approximate reservoir fluid pressure distribution. In our model, fluid viscosity, density and J-T coefficient vary as functions of pressure and temperature.

Three pressure models have been used in this research and they are discussed below. The models give reasonable approximates for pressure in transient flow, pseudo-steady state flow and steady state flow. Although these models are for isothermal flow, they work well with our proposed temperature model.

2.2.1 Flow during Transient Period

The diffusivity equation describes the pressure profile in an infinite-acting, radial reservoir with a slightly compressible and constant viscosity fluid. This equation by Carslaw and Jaeger (1959) is used widely across all sectors of engineering and has the following form:

$$\frac{\partial^2 p}{\partial r^2} + \frac{1}{r}\frac{\partial p}{\partial r} = \frac{\emptyset \mu c_t}{k}\frac{\partial p}{\partial t} \quad (2.2)$$

where p is reservoir pressure, μ is fluid viscosity, c_t is total compressibility of the reservoir, k is reservoir permeability, r is radial distance from the wellbore, and t is time after the start of production.

It's generalized solution:

$$p(r,t) = p_i + \frac{q\mu}{4\pi kh} Ei(-x) \quad (2.3)$$

Where Ei is the exponential integral and x is given by

$$x = \frac{\emptyset \mu c_t r^2}{4kt} \quad (2.4)$$

The line source solution to the diffusivity equation during infinite acting radial flow or transient period is given by Matthews and Russell (1967):

$$p(r,t) = p_i + 70.6\frac{qB_o\mu}{kh} Ei(-\frac{948\emptyset \mu c_t r^2}{kt}) \quad (2.5)$$

All the parameters are in oilfield units such as pressure, p is in psia, flowrate q is in STB/D, μ is in cp, permeability, k is in md, radius r is in ft and time, t is in hours. This solution is an accurate approximation to more exact solutions to the diffusivity equation for

$$3.76 \times 10^5 \frac{\emptyset \mu c_t r_w^2}{k} < t < 948\frac{\emptyset \mu c_t r_e^2}{k}$$

For larger times, the reservoir boundaries affect the pressure distribution in the reservoir, so the reservoir is no longer infinite acting.

Skin factor

Hawkin's showed that if the permeability of the altered zone is k_s and radius is r_s, the additional pressure drop is

$$\Delta p_s = 141.2\frac{qB\mu}{k_s h}\ln\left(\frac{r_s}{r_w}\right) - 141.2\frac{qB\mu}{k_s h}\ln\left(\frac{r_s}{r_w}\right) = 141.2\frac{qB\mu}{kh}\left(\frac{\mathrm{k}}{\mathrm{k_h}} - 1\right)\ln(\frac{r_s}{r_w}) \quad (2.6)$$

Combining eq 2.5 and 2.6,

$$p_i - p_{wf} = -70.6\frac{qB_o\mu}{kh}Ei\left(-\frac{948\emptyset\mu c_t r^2}{kt}\right) + \Delta p_s$$

$$= -70.6\frac{qB_o\mu}{kh}\left[Ei\left(-\frac{948\emptyset\mu c_t r^2}{kt}\right) - 2S\right] \quad (2.7)$$

Here $S = \left(\frac{\mathrm{k}}{\mathrm{k_h}} - 1\right)\ln(\frac{r_s}{r_w})$ (2.8)

If a well is centered in a cylindrical drainage area of radius r_e, then the time required for stabilization t_s, is

$$t_s = 948\frac{\emptyset\mu c_t r_e^2}{k} \quad (2.9)$$

2.2.2 Flow during Pseudo-steady State Period

For the constant rate flow of a well centered in its drainage area of radius re, boundaries begin to affect the pressure drawdown at the well at t=948 $(\emptyset\mu c_t r_e^2)/k$.

Raghavan (1993) proposed a rigorous analytical solution of diffusivity equation for single-phase constant rate liquid production to estimate reservoir pressure as a function of space and time during pseudo-steady state flow regime. He presented that at a large time, the dimensionless solution for reservoir pressure during pseudo-steady state flow is

$$p_D(r_D, t_D) = s + \frac{2}{(r_{eD}^2-1)}\left(t_D + \frac{r_D^2}{4}\right) - \frac{r_{eD}^2}{(r_{eD}^2-1)}\ln r_D - \frac{3r_{eD}^4 - 4r_{eD}^3\ln r_{eD} - 2r_{eD}^2 - 1}{4(r_{eD}^2-1)^2} \quad (2.10)$$

where $t_D = \frac{0.0002637kt}{\emptyset\mu c_t r_w^2}$ (2.11)

$$r_D = \frac{r}{r_w} \quad (2.12)$$

$$p_D(r_D, t_D) = \frac{kh}{141.2qB_o\mu}[p_i - p(r,t)] \quad (2.13)$$

2.2.3 Flow during steady state

Steady-state performance means that all parameters, including flow rate and all pressures, do not vary with time. For a vertical well draining a region with radius re, this means that well boundary pressure pe and the bottomhole flowing pressure pwf are constant when pressure maintenance is present. Pressure maintenance can be done by natural water influx from an aquifer or by water injection. Waterflooding operation and reservoirs with strong gas cap are scenarios where steady-state flow can be used (Economides et al, 2013).

The steady-state performance relationship can be obtained from Darcy's law.

$$q = -\frac{kA}{\mu}\frac{\partial p}{\partial r} \quad (2.14)$$

Here A is cross-sectional area. For a well within a reservoir at a distance r, the flow area is given by $2\pi rh$. Therefore, eq. 2.14 becomes

$$q = -\frac{2\pi rhk}{\mu}\frac{\partial p}{\partial r} \quad (2.15)$$

For constant rate production where reservoir and fluid properties are assumed to be constant, the solution to Eq.2.15 is

$$p(r,t) = p_i - 141.2\frac{qB_o\mu}{kh}\ln(\frac{r_e}{r}) \quad (2.16)$$

All parameters in Eq. 2.16 are in oilfield units.

CHAPTER III

MODEL VALIDATION

App (2010) used a rigorous numerical approach to simulate transient temperature rise of oil as it flowed toward a well at the center of a circular reservoir. Chevarunotai et al (2015) developed an analytical expression for the same system with excellent agreement with App's (2010) numerical simulation. We used results from Chevarunotai et al (2015) to validate our analytical model. Specifically, we compared our temperature estimates with those of Chevarunotai et al. for three different scenarios of the same data set. These three comparisons include:

(1) For a particular production rate estimated temperature as a function of radial distance and time;

(2) For a given time, temperature distribution from reservoir boundary to the wellbore evaluated for different production rates, and

(3) Bottomhole fluid temperature evaluated for different flow rates over time.

3.1 Actual Field Well and Reservoir Data

Table 1 shows the reservoir properties of a reservoir which is considered as the base case for the flowing oil temperature calculation. These are the same as the data set shown by App (2010).

Table 1: Reservoir parameters of an actual reservoir used in the study by App (2010)

Parameter, unit	**Value**
Permeability, md	20
Porosity, %	25
Thickness, ft	100
Initial Pressure, psia	21,000
Bubble Point Pressure, psia	7,000
Rock Compressibility, psi^{-1}	$3 \cdot 10^{-6}$
Initial Temperature, °F	302
Wellbore Radius, ft	0.41
Reservoir Outer Radius, ft	4,000
Irreducible Water Saturation, %	15
Reservoir Heat Transfer Coefficient, $BTU/hr \cdot ft^2 \cdot °F$	0.92

Reservoir fluid properties are shown in Table 2.

Table 2: Reservoir fluid parameters of an actual reservoir used in the study App (2010)

Parameter, unit	Value
Oil Formation Volume Factor, bbl/STB	1.05
Fluid Density – oil , lbm/ft^3	51.19
Specific Heat Capacity - oil, BTU/lbm·ft	0.53
Joule-Thompson throttling coefficient - oil, °F /psi	-0.0055
Fluid Density – water , lbm/ft^3	63.68
Specific Heat Capacity - water, BTU/lbm·ft	1.0
Joule-Thompson throttling coefficient - water, °F /psi	-0.0024
Density – formation , lbm/ft^3	165.43
Specific Heat Capacity – formation, BTU/lbm·ft	0.20
Thermal Conductivity, BTU/ hr·ft·°F	1.73

3.2 Case Study 1: Temperature Distribution with Time at a Constant Production Rate

Fig. 2 shows evaluated temperatures for various producing times for a constant production rate of 6200 STB/D. The dotted lines represent results from Chevarunotai et al. (2015) model. Our estimates, represented by solid lines, are in good agreement with those of Chevarunotai (2015); varying at most by 2 ^{O}F. We attribute the differences in

estimates to the fact that Chevarunotai et al (2015) model does not allow for density and J-T coefficient to vary with pressure and temperature as the oil moves towards the wellbore. Note that the solid curves for Fig. 2 (as well as those in Figs. 3 and 4) were generated using a density of 51.1 lbm/ft^3 and J-T coefficient of 0.00289 ^{o}F/psi at the reservoir boundary and were allowed to vary in the radial direction as pressure and temperature changed. Flowing from reservoir boundary to the wellbore, oil density decreased by about 6% as the J-T coefficient increased by 2.6% for 100 days of production.

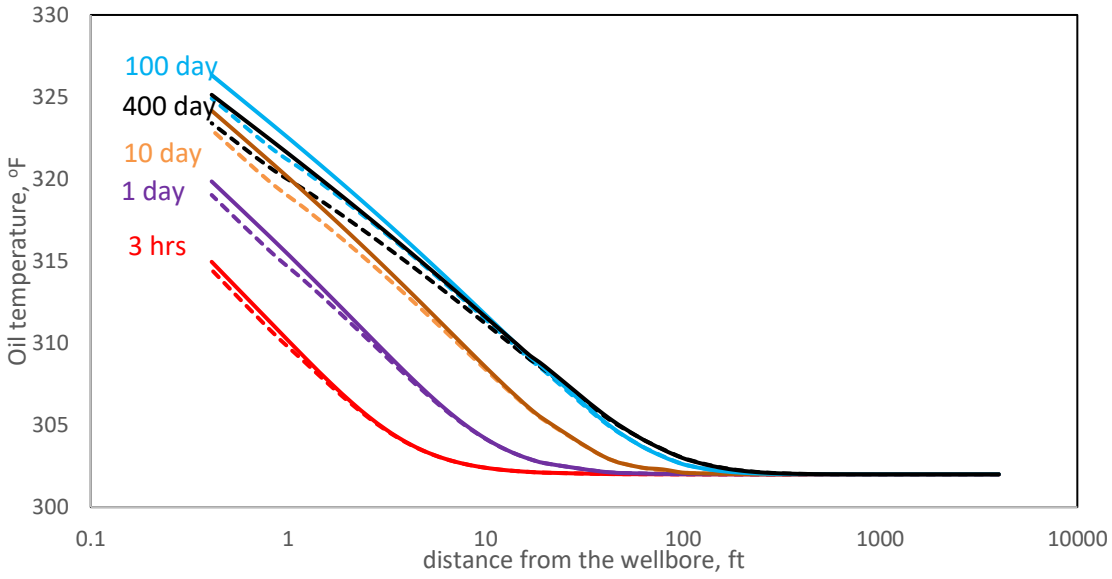

Fig. 2: Analytical model results in good agreement with Chevarunotai et al. (2015) solutions at different production times.

We observe that oil temperature in most of the formation remains unaffected; temperature increase is only noticeable up to about 100 ft from the wellbore for long producing times. This is because most of the pressure drop occurs near the wellbore, and

pressure drop causes temperature rise. In addition, it is obvious that longer producing time produces more heat, leading to greater temperature rise with producing time. However, Fig. 2 shows that the rate of temperature increase slows down with time, and finally the reversal occurs. Therefore, the fluid temperature rise for 400 days (black lines) of production is less than that for 100 days (blue lines). This reversal is captured in both Chevarunotai et al. (2015) and our analytical solutions. The reason for this reversal is that much longer production leads longer period of heat loss as well as reduction of pressure drop due to lower viscosity leading to lower temperature rise.

3.3 Case Study 2: Temperature Distribution at Different Rates

We ran our analytical model at five different flow rates ranging from 970 to 6,200 STB/D for 50 days of production. The results are shown in **Fig. 3**, with our estimates in solid lines, while those of Chevarunotai et al. (2015) in dotted lines. Good agreement between estimates of our analytical model with those of Chevarunotai et al.(2015) model, is again evident. Additionally, Fig. 3 shows that, as expected, the temperature rise is higher for higher production rates.

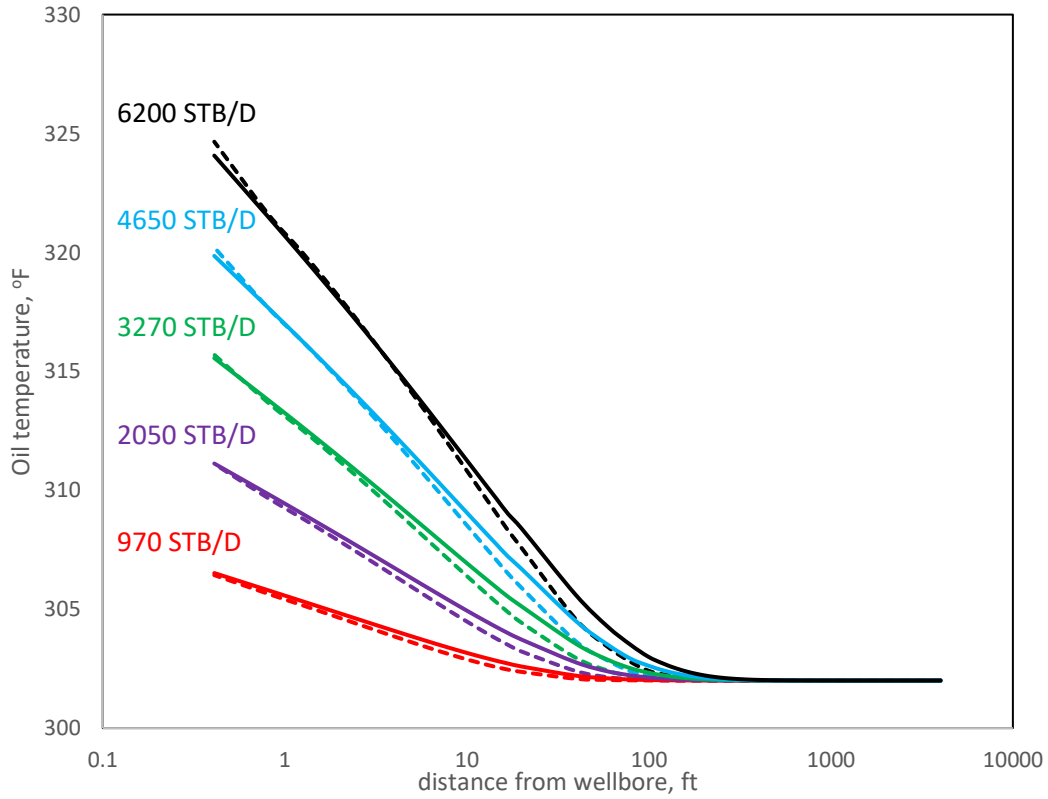

Fig. 3: Analytical model compares well with Chevarunotai et al. (2015) model at different flowrates.

3.4 Case Study 3: Bottomhole Temperature at Different Rates

At five different flowrates, the bottomhole flowing temperature is calculated from the analytical model and compared with App's values in **Fig. 4**.

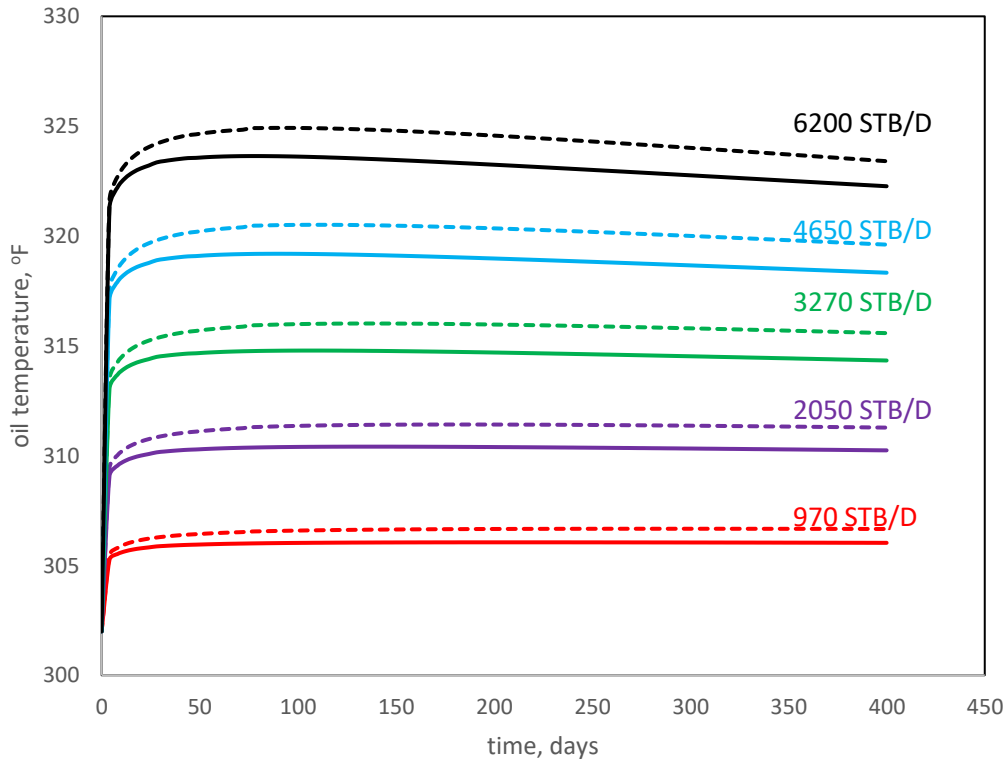

Fig. 4: Good agreement between analytical model results with those of Chevarunotai et al. (2015) model for bottomhole temperature**.**

Fig. 4, similar to Figs. 2 and 3, clearly indicates that the assumptions made to arrive at the analytical solution are quite robust. An accurate analytical solution like the one we have developed saves computational time and offers the advantage of quick adoption in other simulations where the fluid entrance temperature to the well need to be estimated from reservoir temperature. Estimates from this analytical solution could be effectively used in estimating zonal rate contribution from temperature data.

We note that the our analytical model requires various reservoir and fluid properties data. To understand the importance of input parameters, we performed a sensitivity analysis of our temperature estimates in the next section.

CHAPTER IV

SENSITIVITY ANALYSIS

We performed various simulations to determine the effect of viscosity, reservoir permeability, Joule-Thompson coefficient, density, oil formation-volume factor, and reservoir coefficient of heat transfer (to the over- and under-burden). A rigorous sensitivity analysis permits us to have an improved understanding of the impact of these variables and their relative importance in temperature evaluation. For consistency, all the sensitivity analysis were conducted at a constant production rate of 6,200 STB/D and generally after 50 days of production.

4.1 Fluid Viscosity

Higher oil viscosity is expected to create to higher pressure gradient that would lead to larger temperature gain as oil flows towards the wellbore. To observe this effect of viscosity on fluid temperature, we ran simulations for three different values of oil viscosities ranging from 1.5 to 3 cp. In these simulations, viscosity was held constant over the entire reservoir for each case. Fig. 5 clearly shows that fluid temperature rise due to J-T heating significantly depends on oil viscosity. Blue lines in this figure show oil temperature for three hour production period, while those for 100 days of production are shown in orange. As the figure shows, temperature increase is higher for higher viscosity oil for the same production period than for lower viscosity oil. Similarly, for higher producing time, that allows greater J-T heat generation, the differences in temperature rise for oil of differing viscosities is greater than for the same oil for lower producing time. We emphasize that these simulations reflect those with oil viscosity remaining constant

for a given simulation. As it was pointed out while discussing Fig. 2, when oil viscosity is allowed to vary with oil movement from the reservoir toward the wellbore, the coupled nature of temperature, pressure, and the resultant viscosity change can complicate the picture.

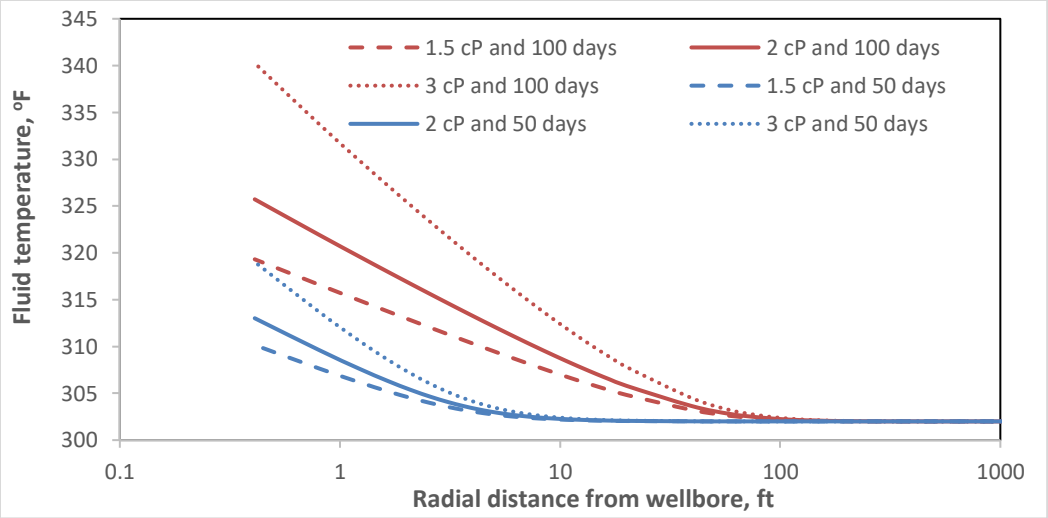

Fig. 5: Flowing-fluid temperature distributions with different fluid viscosities after 50 and 100 days

4.2 Permeability

The J-T effect leading to temperature increase, is dependent on the pressure gradient and oil's J-T coefficient. Therefore, for formations with lower permeability leading to higher pressure gradient, oil temperature rise will be greater than for a higher permeability reservoir, everything else remaining constant. As we can see from Fig. 6—it makes this point by showing the estimated oil temperature after 50 days of production at 6,200 STB/D for three different reservoir permeability.

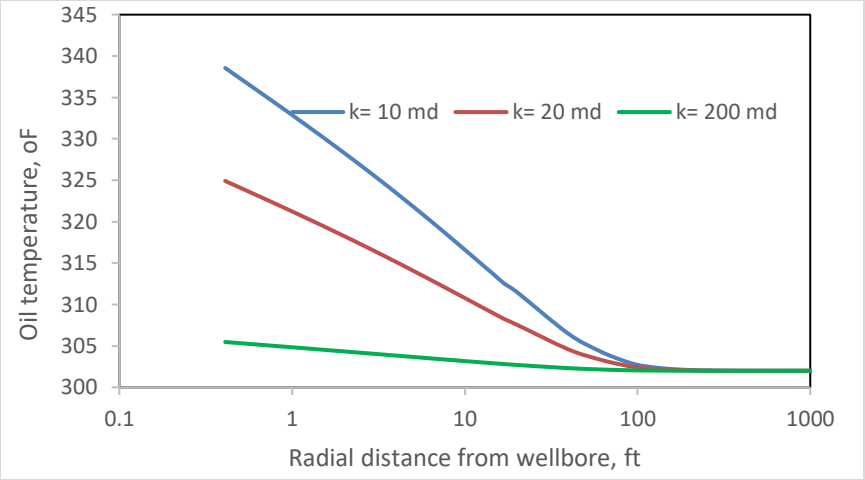

Fig. 6: Decreasing permeability lead to higher-pressure gradients resulting in increased temperature

4.3 Joule-Thompson Coefficient

Higher Joule-Thompson coefficient implies higher heating; consequently, Fig. 7 shows increasing the increasing temperature trend.

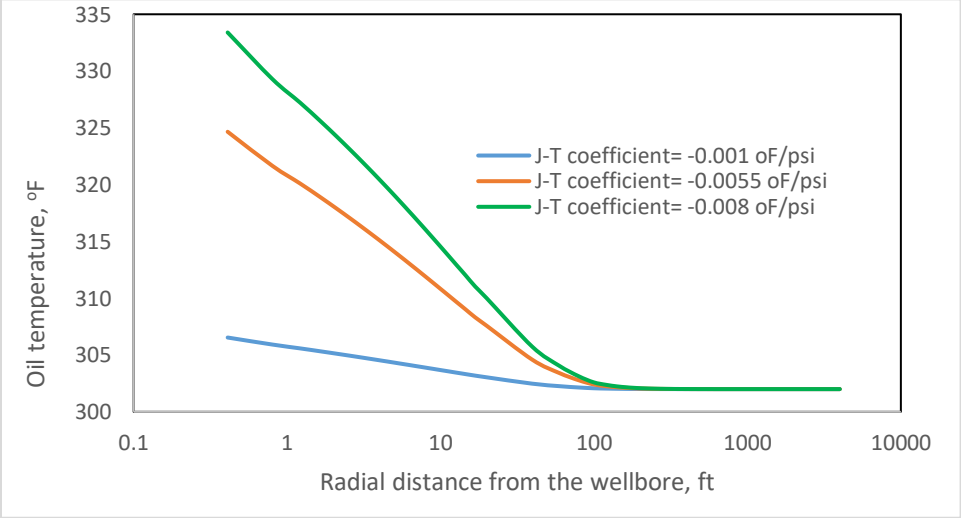

Fig. 7: Sensitivity of oil temperature to Joule-Thompson coefficient at an oil rate of 6,200 STB/D after 50 days.

4.4 Other Factors

Among other parameters that can possibly influence fluid heating, we examined the effect of heat transfer (to over- and under-burden) coefficient, h_c. We found that even for more than an order of magnitude increase (from 0.1 to 2.5 Btu/ (hr-ft-^{o}F) in the heat-transfer coefficient, oil temperature went down by a maximum of less than 3^{o}F. Although higher h_c leads to greater heat loss and the consequent lower fluid temperature, the effect appears minimal. Given that an accurate value of h_c is generally unavailable, this finding is reassuring.

Our simulations show that the effect of other variables, such as oil formation-volume factor, reservoir radius, and fluid density, do not have any appreciable effect on oil heating. Note that the value of oil J-T coefficient depends primarily on oil density, and secondarily on variation of oil density with temperature. We also conducted the sensitivity analysis for a low flow rate (500 STB/D), which is given in Appendix A to avoid repetitiveness. As expected, fluid temperature changes very little when in a low-rate environment.

4.5 Statistical Design of Experiments

To understand the relative influence of various independent variables on the dependent variable reservoir temperature, we conducted design of experiments (DoE). The six independent variables include permeability, reservoir radius, oil-formation volume factor, Joule-Thompson coefficient, and overall heat-transfer coefficient.

In our DoE, calculations reflect oil temperature at three different locations; that is, at the wellbore, and at 10 ft and 100 ft from the wellbore. All these temperatures have been determined at a production rate of 6,200 STB/D after 50 days of production. Figs. 8 through 10 present these Pareto charts.

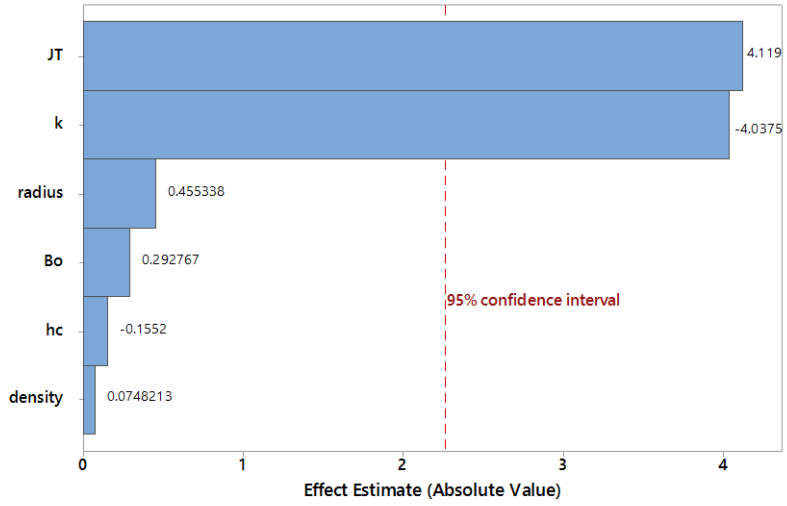

Fig. 8: Pareto chart for fluid temperature at the wellbore.

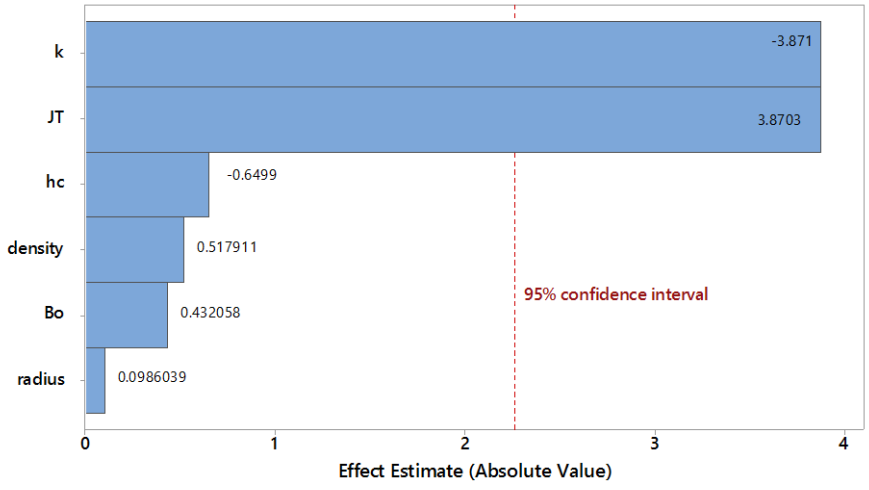

Fig. 9: Pareto chart for fluid temperature at 10 ft from the wellbore.

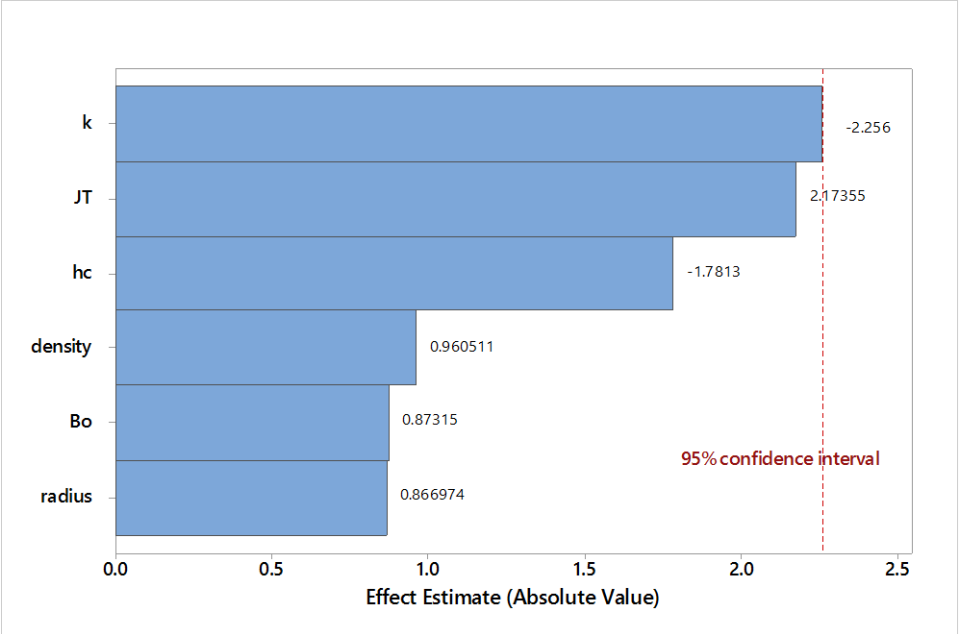

Fig. 10: Pareto chart for fluid temperature at 100 ft from the wellbore.

These Pareto charts indicate that reservoir permeability and the J-T effect are the most important independent variables for the estimation of flowing-fluid temperature, particularly at the wellbore. The closer the fluid gets to the wellbore, the effect of other variables tend to diminish. In contrast, Fig. 10 shows that at 100 ft from the wellbore, none of the independent variables have any statistical significance on fluid temperature because of minimal J-T effect. Figs. 2 and 3, among others, substantiate this notion.

On a Pareto chart, the *x*-axis represents the student's *t*-values and the *y*-axis the independent variables. Details can be found in a statistics textbook, such as that by Montgomery (2012). Let us point out that the negative value associated with a variable suggests that its increase has an adverse impact on the dependent variable, fluid temperature; whereas, the opposite is true for a positive value. In other words, Fig. 8

through Fig. 10 suggest that the fluid temperature increases with decreasing reservoir permeability but with increasing J-T coefficient.

We also developed a tornado chart for a constant production time of 50 days to analyze the sensitivity of flowing-fluid temperature, as shown in Fig. 11. This chart reaffirms that the four primary independent variables are flow rate, permeability, viscosity, and J-T coefficient.

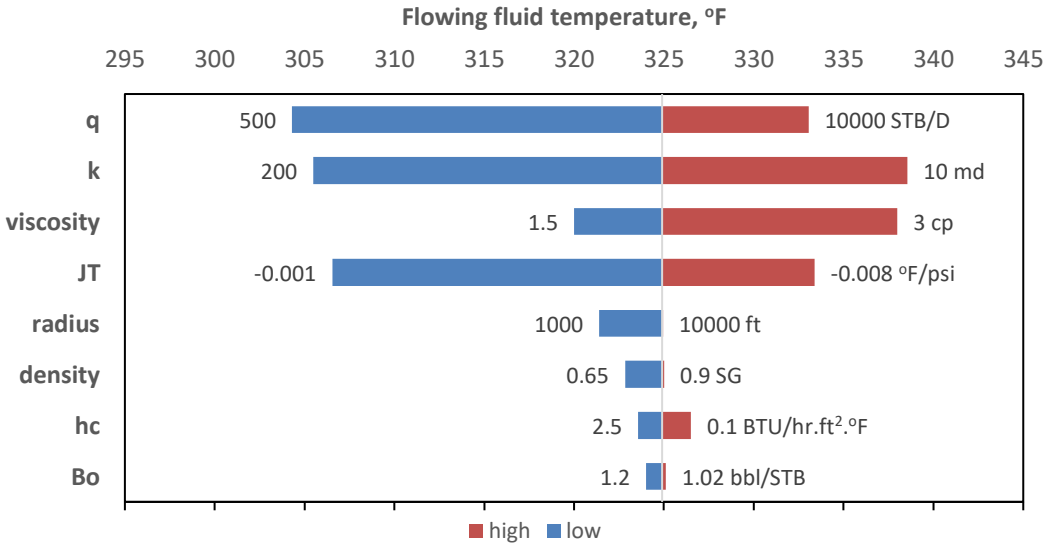

Fig. 11: Tornado chart showing the effect of these parameters on temperature distribution.

CHAPTER V

WELLBORE MODEL

For our analytical temperature model, we can get the bottom-hole temperature and pressure for a well. In order for an analysis of complete production system, we can couple our model with a wellbore heat transfer model.

5.1 Wellbore Heat Transfer Model

We are using an existing wellbore heat transfer model to couple with our reservoir model. Among the wellbore heat transfer models in use, the temperature model by Hasan et al (2009) is noteworthy. This is an analytical model for computing wellbore fluid temperature in steady state flow. This model takes into account Joule-Thomson coefficient and fluid expansivity. The approach taken in this model divides the wellbore into several sections of uniform thermal property. It also takes into account height of seawater.

5.1.1 Analytical Expression for T_f

The differential equation for fluid temperature from Hasan et al (2009):

$$\frac{dT_f}{dz} = \pm L_R\left(T_f - T_{ei}\right) + \frac{gsin\alpha_i}{c_p J g_c} - \phi \tag{5.1}$$

Here the variable ϕ represents the kinetic-energy and also contains Joule-Thomson coefficient.

$$\phi = \frac{V}{c_p J g_c}\frac{dV}{dZ} - C_J\frac{dp}{dZ} \tag{5.2}$$

The solution for Eq. 5.1 is

$$T_f = T_{ei} + 1 - \frac{e^{(z-z_j)L_R}}{L_R}\left(g_G sin\alpha + \phi - \frac{gsin\alpha}{c_p}\right) + e^{(z-z_j)L_R}(T_{fi} - T_{ei}) \tag{5.3}$$

Here T_{ei} represents undisturbed earth or sea temperature far away from the well. We are calculating T_{ei} from our reservoir model.

5.2 Model Validation with Data

We coupled our reservoir model with the wellbore model by Hasan (2009). From our reservoir model, we can calculate bottomhole pressure and temperature. We used those values as input in wellbore temperature model.

We used the following field well and reservoir data for validating our model.

Table 3: Well and reservoir data

Parameter, unit	Value
Permeability, md	10
Porosity, %	18
Thickness, ft	370
Initial Pressure, psia	19,400
Bubble Point Pressure, psia	6,000
Rock Compressibility, psi^{-1}	$3 \cdot 10^{-6}$
Initial Temperature, °F	227
Wellbore Radius, ft	0.41
Reservoir Outer Radius, ft	4,000
Irreducible Water Saturation, %	38
Well TVD, ft	20000
Sea Level, ft	5000

Table 4 shows the fluid properties used for our calculation:

Table 4: Fluid properties used for calculation

Parameter, unit	Value
Fluid Density – oil , API	26.5
Oil density, g/cc	0.895
Oil Viscosity, cp	5.6
Gas Gravity, g/cc	0.9
Formation GOR, scf/STB	220
Specific Heat Capacity - water, BTU/lbm·ft	1.0
Joule-Thompson throttling coefficient - water, °F /psi	-0.0024

We plotted the bottomhole hole pressure and temperature values with time at different rates to match with field data. Then we plotted another graph showing wellhead pressure and temperature. As we can see from the figures, temperature and pressure match accurately with the field data. The field data is for different flow rates and times and those were inputs in reservoir model.

In the following figures, dotted line represent field data and the solid lines represent values from the temperature model. In Fig. 12, we plotted bottomhole pressure and temperature with time.

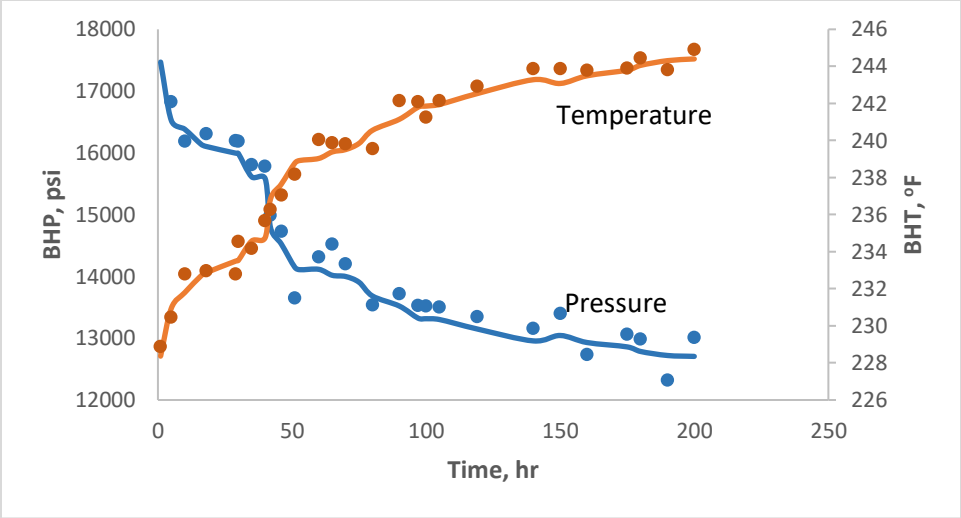

Fig. 12: Bottomhole pressure and temperature with time

Using these values from our reservoir model, we plot them in wellbore model by Hasan et al (2009). The wellhead pressure and temperature plots against time can be seen from Fig. 13.

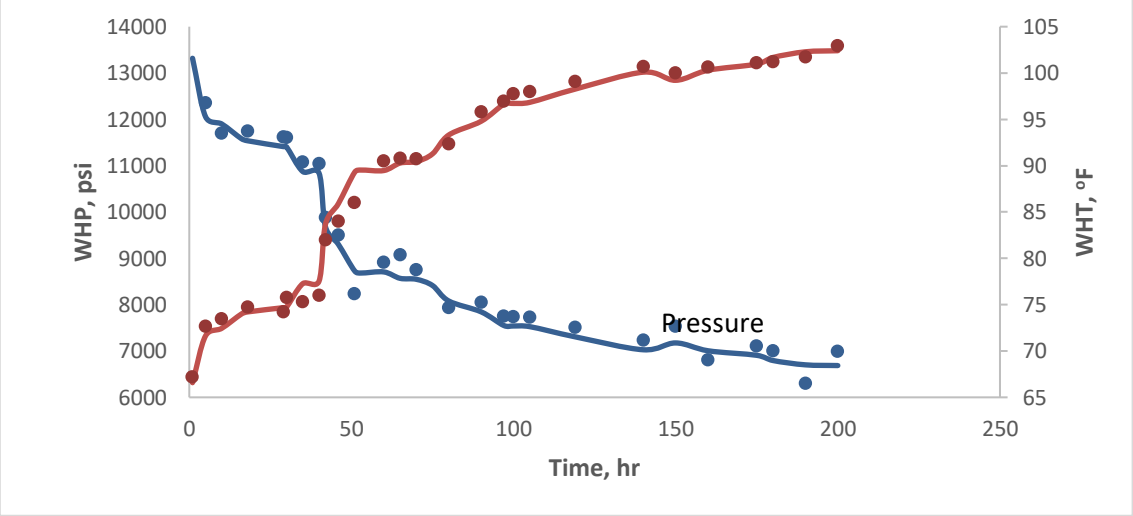

Fig. 13: Wellhead pressure and temperature with time

We also plotted temperature profile along the depth of the well in Fig. 14. The field data is for an offshore well where mudline is 5000 ft below sea level.

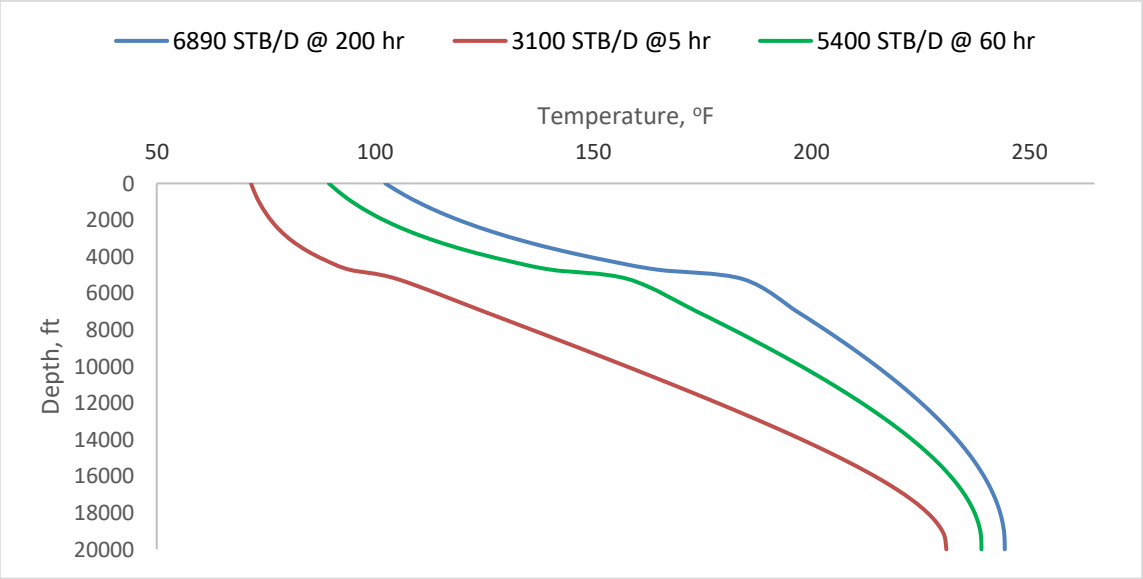

Fig. 14: Wellbore temperature profile

As we can see from the figure, for low flow rates at earlier times, the temperature drops quickly. As production time keeps increasing, temperature at bottomhole is higher and so wellhead temperature also increases.

CHAPTER VI

MODEL APPLICATION FOR GAS

Non ideal behavior of fluid volume with respect to pressure and temperature is the reason behind Joule-Thomson effect. For ideal gas, there is no J-T effect. Same for liquid, as J-T coefficient is inversely proportional to density, for constant density fluid, there would be no Joule-Thomson phenomena. The effect of J-T happens only when deviation from ideal behavior happens. We can expand our temperature model built for single-phase oil to single-phase gas by taking into account gas properties.

6.1 Gas Properties Calculation

In order to make our model suitable for gas temperature calculation, we made several modifications. The gas properties were included in the model and we allowed several properties to vary. These properties include gas viscosity, gas density, J-T coefficient and z-factor.

6.1.1 Gas viscosity

Gas viscosity correlations have been presented by a number of authors. For our calculations, we used the one of Lee, Gonzales and Eakin (1966):

$$\mu_g = A(10^{-4})EXP(B\rho_g^c) \tag{6.1}$$

Where:

$$A = \frac{(9.379+0.01607M_a)T^{1.5}}{209.2+19.26M_a+T} \tag{6.2}$$

$$B = 3.448 + \frac{986.4}{T} + 0.01009M_a \tag{6.3}$$

$$C = 2.447 - 0.2224B \tag{6.4}$$

ρ_g is gas density in gm/cc, M_a is apparent molecular weight, and T is the temperature in Rankin and μ_g is gas viscosity in cp.

6.1.2 Gas Density

Gas density is calculated from ideal gas law.

$$pV = ZnRT = \frac{ZWRT}{M_a} \tag{6.5}$$

$$\rho = \frac{pM_a}{ZRT} = \frac{0.00149406M_a}{RT} \tag{6.6}$$

Where ρ is gas density in gm/cc, M_a is apparent molecular weight, T is temperature in ^oR and p is pressure in psi.

6.1.3 J-T coefficient

An expression for calculating Joule-Thompson coefficient for real gases has been developed by Hasan et al (2009).

$$v = \frac{zRT}{p} \tag{6.7}$$

$$\left(\frac{\partial V}{\partial T}\right)_p = \left(\frac{ZR}{p}\right) + \left(\frac{RT}{p}\right)\left(\frac{\partial Z}{\partial T}\right)_p = \left(\frac{V}{T}\right) + \left(\frac{V}{Z}\right)\left(\frac{\partial Z}{\partial T}\right)_p \tag{6.8}$$

$$\text{Hence, } c_p C_J = \left(\frac{VT}{Z}\right)\left(\frac{\partial Z}{\partial T}\right)_p \tag{6.9}$$

The details of the calculation are given in the appendix C.

6.2 Properties for Low Pressure Gas DST

The following properties are taken from App (2009) for temperature analysis of a low-pressure gas production test. They are shown in table 5 and 6.

Table 5: Reservoir and fluid properties (App, 2009)

Parameter	Value	Parameter	Value
k, md	3.5	T_i, °F	376
Porosity, %	15	r_w, ft	0.41
Thickness, ft	20	r_e, ft	4000
p_i, psia	3880	S_w, %	15
p_d, psia	650	$B_g@p_i$, rb/mcf	1.063
c_r, psi^{-1}	$3E^{-6}$	c_w, psi^{-1}	$3E^{-6}$

Table 6: Component thermal and physical properties

Properties	Gas	Water	Rock
ρ, lbm/ft^3	11.58	62.43	165.0
c_p, Btu/lbm-°F	0.52	1.00	0.23
β, 1/°F	4E-4	5E-4	5E-4
μ_{JT}, °F/psi		-0.0024	
λ_t, Btu/hr-ft-°F	1.6		

6.3 Flowing Fluid Temperature at Constant Flow Rate

We plotted the temperature from reservoir boundary to wellbore with a constant flowrate of 3300 MSCF/D at 24 hr. The reservoir boundary pressure is 3880 psia. The Joule-Thomson expansion coefficient for low pressure gas is positive-so it results in a decrease in temperature. The cooling effect is observed as it flows from the reservoir boundary to wellbore as we can see in Fig. 15:

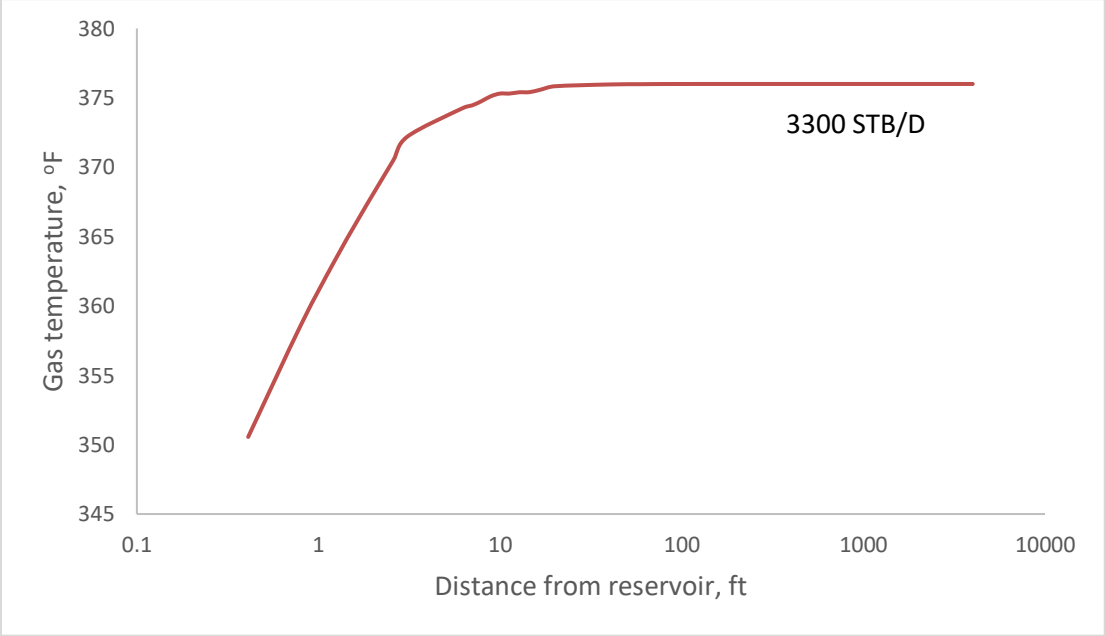

Fig. 15: Temperature drop for gas at 3300 MSCF/D as it flows from reservoir boundary to wellbore

6.4 Bottomhole Temperature with Time

We also plotted the bottomhole temperature for low pressure gas with time. We tried to match those with data from App (2009). The dotted line represents the data and the solid line represents the temperature estimated from our model. As we can see clearly

from Fig. 16, after a production time of 12 hrs, our model predicts a 22 ^{o}F temperature reduction. It's due to J-T cooling.

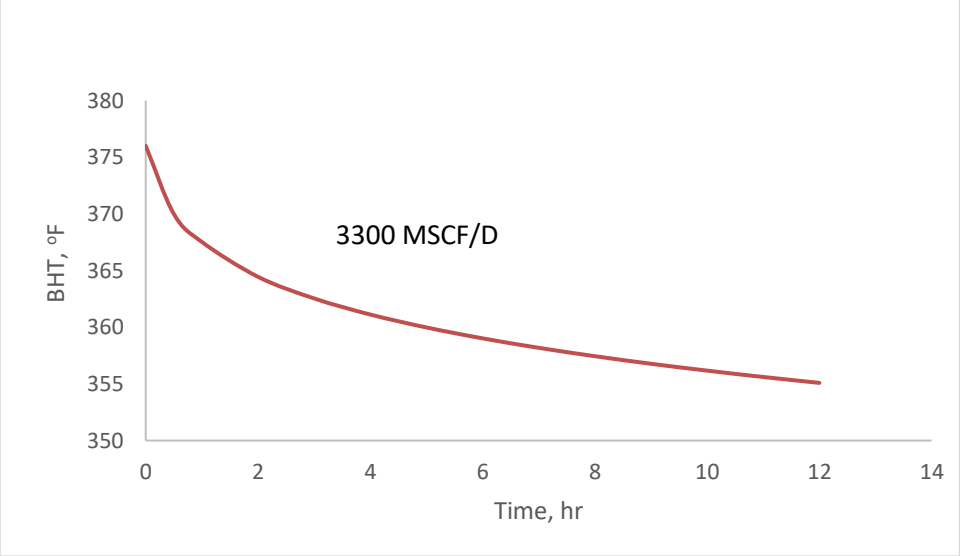

Fig. 16: Cooling of gas with time as bottomhole with a rate of 3300 MSCF/D

These cases illustrate non-isothermal behavior of gas due to Joule-Thompson expansion. These become highly noticeable when there is high drawdown as Joule-Thomson effects become more prominent.

CHAPTER VII

CONCLUSION AND RECOMMENDATIONS

7.1 Conclusions

This study shows that the flow rate plays a major role in the assessment of fluid temperature vis-à-vis viscosity due to the J-T effect. Therefore, the early assessment of fluid's PVT properties and their dependence on pressure and temperature are critically important for the calculations of well performance predictions. For example, viscosity decrease with increasing temperature, a consequence of increasing rate, can potentially increase the well productivity index (PI) in a significant way. Because PI is inversely proportional to viscosity, the improved well performance occurs with increasing drawdown within permissible limits of completion and tubular integrity.

Given the importance of radial permeability within a well's 100 ft radius, pressure-transient testing appears to be a logical source for this information. If specific transient tests are unavailable, the proposed model can be run in an inverse mode to estimate permeability with accurate inputs of fluid, completion, and relevant parameters.

The significant increase in temperature at the wellbore with increased drawdown suggests that tubular design must account for sustained temperature plateau in the early life of an asset when high rates are maintained. Annular pressure buildup due to heating of annular fluid may limit production rates unless the unusual increase of 25 ^{o}F or higher is anticipated and accounted for in design calculations. This model allows one to facilitate such calculations with limited data in a probabilistic frame even before the drilling occurs during the early stage of field development.

1. An improved analytical model for estimating the flowing fluid temperature at the wellbore has been developed when production occurs at large drawdowns in low-permeability reservoirs for fluids with moderate viscosity. Unlike its predecessor, this model allows variation of oil density, viscosity, and the J-T coefficient with pressure and temperature. Specifically, we offer a thermodynamically robust expression for calculating the J-T coefficient based on the fluid's PVT properties.
2. The sensitivity analysis showed that the fluid temperature increases with decreasing permeability, increasing fluid viscosity, flow rate, and the J-T coefficient.
3. Heating, induced by the J-T effect, is restricted to about 100 ft away from the wellbore. The low fluid velocity is primarily responsible for this phenomenon.
4. Bottomhole flowing-fluid temperature from the analytical reservoir model is further coupled with wellbore heat-transfer model to estimate flowing-fluid temperature along the wellbore to the surface. The flowing-fluid temperature along the wellbore is helpful for well designing and production optimizing.
5. An inverse calculation of flow parameters like flowrate, reservoir permeability can be done from coupled reservoir/wellbore model.
6. Our analytical temperature model is further extended to study gas temperature in reservoir.

7.2 Recommendations for Further Work

In this study, a rigorous analytical temperature model was developed which allows for fluid property variation. It was coupled with a wellbore heat transfer model and validated

with data. This model can be used to futher investigate more complex flow problems and the scopes for further research is given below:

1. Validate reservoir gas temperature with field data.
2. Perform an analysis for two-phase flow
3. Make adjustments to accommodate for fluid injection in reservoir.
4. Evaluate the impact of pressure-transient term to see the significance of this term during two-phase flow.

REFERENCES

App, J.F. 2009. Field Cases: Nonisothermal Behavior Due to Joule-Thomson and Transient Fluid Expansion/Compression Effects. Paper presented at the SPE Annual Technical Conference and Exhibition, New Orleans, Louisiana, 50-63.

App, J.F. 2010. Nonisothermal and Productivity Behavior of High-Pressure Reservoirs. *SPE Journal* **15** (1): 50-63.

App, J.F., Yoshioka, K. 2013. Impact of Reservoir Permeability on Flowing Sandface Temperatures: Dimensionless Analysis. *SPE Journal* **18** (4): 685-694.

Carslaw, H.S., Jaeger, J.C. 1959. *Conduction of Heat in Solids*, 2nd edition. Oxford, Clarendon Press.

Chevarunotai, N. 2014. Analytical Models for Flowing-Fluid Temperature Distribution in Single-Phase Oil Reservoirs Accounting for Joule-Thomson Effect. Masters, Texas A & M University.

Chevarunotai, N., Hasan, A.R., Kabir, C.S. 2015. Transient Flowing-Fluid Temperature Modeling in Oil Reservoirs for Flow Associated with Large Drawdowns. Paper presented at the SPE Annual Technical Conference and Exhibition, Houston, Texas, USA.

Dindoruk, B., Christman, P.G. 2004. PVT Properties and Viscosity Correlations for Gulf of Mexico Oils. *SPE Reservoir Evaluation & Engineering* **7** (6): 427-435.

Dranchuk, P.M., Purvis, R.A., Robinson, D.B. 1973. Computer Calculation Of Natural Gas Compressibility Factors Using The Standing And Katz Correlation. Paper presented at the Petroleum Society of Canada Annual Technical Meeting, Edmonton, May 8 - 12.

Duru, O.O., Horne, R.N. 2010. Modeling Reservoir Temperature Transients and Reservoir-Parameter Estimation Constrained to the Model. *SPE Reservoir Evaluation & Engineering* **13** (06): 873-883.

Economides, M.J., Hill, A.D., Ehlig-Economides, C. et al. 2013. *Petroleum Production Systems*, 2nd edition, 20-65, Prentice Hall.

Hasan, A.R., Kabir, C.S., Wang, X. 2009. A Robust Steady-State Model for Flowing-Fluid Temperature in Complex Wells. *SPE Production & Operations* **24** (2): 269-276.

Izgec, B., Kabir, C.S., Zhu, D. et al. 2007. Transient Fluid and Heat Flow Modeling in Coupled Wellbore/Reservoir Systems. *SPE Reservoir Evaluation & Engineering* **10** (03): 294-301.

Lauwerier, H.A. 1955. The transport of heat in an oil layer caused by the injection of hot fluid. *Applied Scientific Research, Section A* **5** (2): 145-150. http://dx.doi.org/10.1007/BF03184614.

Lee, A.L., Gonzalez, M.H., Eakin, B.E. 1966. The Viscosity of Natural Gases. *Trans AIME* (237): 997-1000.

Matthews, C.S., Russell, D.G. 1967. *Pressure Buildup and Flow Tests in Wells*, Vol. 1. Richardson, Texas: Monograph Series, SPE.

Raghavan, R. 1993. *Well Test Analysis*. Englewood Cliffs, New Jersey, Prentice Hall.

Ramazanov, A.S., Nagimov, V.M. 2007. Analytical Model for the Calculation of Temperature Distribution in the Oil Reservoir during Unsteady Fluid Inflow. *Oil and Gas Business* (1).

Ramazanov, A.S., Nagimov, V.M., Akhmetov, R.K. 2013. Analytical Model of Temperature Prediction for a Given Production History. *Oil and Gas Business* (1): 537-546.

Spillette, A.G. 1965. Heat Transfer During Hot Fluid Injection Into an Oil Reservoir. *PETCO Journal Paper*. 65-04-06 PETCO. http://dx.doi.org/10.2118/65-04-06.

APPENDIX A

ANALYTICAL MODEL

The comprehensive energy-balance equation for the reservoir system described in the main body can be reduced to a first-order, partial-differential equation (PDE) (Chevarunotai, 2014; Chevarunotai et al. 2015):

$$\frac{\partial T}{\partial t} - \frac{B}{Ar}\frac{\partial T}{\partial r} - \frac{C}{Ar^2} = -\frac{D}{A}T + \frac{E}{A} \tag{A.1}$$

Eq. 2, solved using the method of characteristics, led to Eq. 1 reproduced below

$$T(r,t) = T_i + \frac{C}{2B}e^{\frac{H(Ar^2+2Bt)}{2B}}Ei\left[-\frac{H(Ar^2+2Bt)}{2B}\right] - \frac{C}{2B}e^{\frac{HAr^2}{2B}}Ei\left[-\frac{HAr^2}{2B}\right] \tag{A.2}$$

Where

$$A = \left[\emptyset s_o \rho_o c_{po} + \emptyset s_w \rho_w c_{pw} + (1-\emptyset)\rho_f c_{pf}\right]\left(\frac{2\pi h}{q}\right) \tag{A.3}$$

$$B = \rho_o c_{po} \tag{A.4}$$

$$C = \frac{q\rho_o \sigma_o \mu}{2\pi hk} \tag{A.5}$$

$$D = \frac{4h_c\pi}{q} \tag{A.6}$$

$$E = \frac{4h_c\pi}{q}T_i \tag{A.7}$$

$$H = \frac{D}{A} \tag{A.8}$$

The second term on the left side of Eq. A.2 containing the parameter *C* includes fluid convection (through rate, *q*) and J-T heating (through σ). Both terms on the right side involve heat lost by the flowing fluid to the formation (through heat transfer coefficient, *h*). The derivation is available in Chevarunotai (2015)

APPENDIX B

ESTIMATION OF PVT PROPERTIES

While properties in Eq. 1 were assumed to have negligible variation, Eq. A-2 (Eq. 1) allows fluid viscosity, density, and J-T coefficient to vary with pressure and temperature along the flow path.

B.1 Viscosity

To calculate viscosity, oil viscosity data from laboratory measurement was used. The following figure gives viscosity as a function of pressure and temperature.

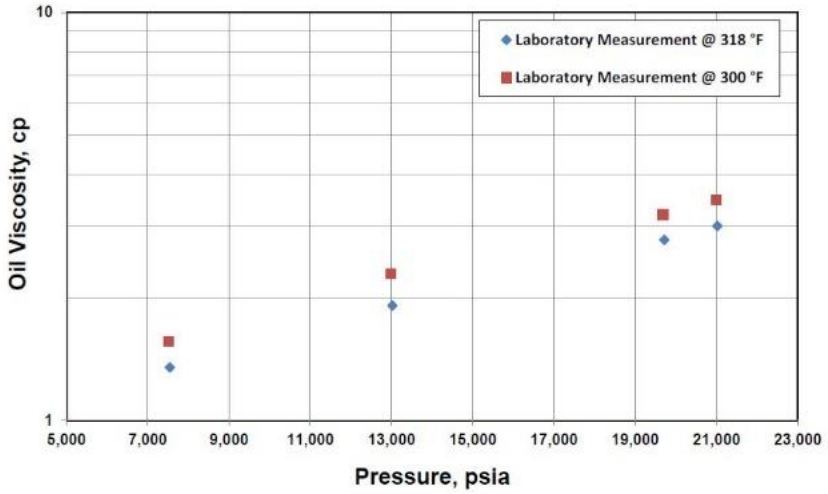

Fig. B.1: Viscosity as a function of pressure and temperature (App, 2010)

B.2 Viscosity Correlation

Dindoruk and Christman (2004) developed another viscosity correlation used in this work. For the development of these corrlations, more than 100 pressure/volume/temperature (PVT) reports from the Gulf of Mexico (GOM) have been used. They tested the correlations with those of Standing and Petrosky.

Dead-Oil-Viscosity Correlation (μ_{oD})

The following equation is developed for calculating dead-oil viscosity:

$$\mu_{oD} = \frac{a_3 T^{a_4} (logAPI)^A}{a_5 p_{bp}^{a^6} + a_7 R_{sbp} a_8} \quad \text{(B.1)}$$

Where $A = a_1 logT + a_2$ (B.2)

Coefficients for Eq. B.1 and Eq. B.2 are given in Table 3.

Table 7: Coefficients for the dead-oil viscosity correlation (Dindoruk and Christman, 2004)

Coefficient (μ_{oD} correlation)	Value
a_1	14.505357625
a_2	-44.868655416
a_3	9.36579 E+09
a_4	-4.194017808
a_5	-3.1461171E-09
a_6	1.517652716
a_7	0.014043365
a_8	-0.000776880

Saturated-Oil viscosity correlation (μ_{obp})

Saturated-oil viscosity correlations require the use of dead-oil viscosity. The following equation was presented by Dindoruk and Christman (2004):

$$\mu_{obp} = A(\mu_{oD})^B \quad \text{(B.3)}$$

Where

$$A = \frac{a_1}{\exp(a_2 R_s)} + \frac{a_3 R_s^{a_4}}{\exp(a_5 R_s)} \quad \text{(B.4)}$$

And

$$B = \frac{a_6}{\exp(a_7 R_s)} + \frac{a_8 R_s^{a_9}}{\exp(a_{10} R_s)} \quad \text{(B.5)}$$

Coefficients for Eq. B.4 and B.5 are given in Table 4.

Table 8: Coefficients of the proposed saturated-oil viscosity correlation (Dindoruk and Christman, 2004)

Coefficient (μ_{obp} correlation)	Value
a_1	1E+00
a_2	4.74079E-04
a_3	-1.023451E-02
a_4	6.600358E-01
a_5	1.075080E-03
a_6	1.00 E+00
a_7	-2.191172E-05
a_8	-1.660981E-02
a_9	4.233179E-01
a_{10}	-2.273945E-04

Unsaturated-Oil Viscosity correlation (μ_o):

Using saturated oil viscosity, the correlation for undersaturated oil is found:

$$\mu_o = \mu_{obp} + a_6(p - p_{bp})10^A \quad \text{(B.6)}$$

Where

$$A = a_1 + a_2 log\mu_{obp} + a_3 log R_s + a_4 \mu_{bop} \log R_s + a_5(p - p_{bp}) \quad \text{(B.7)}$$

Coefficients for Eq. B.6 and B.7 are given in table 5.

Table 9: Coefficients for the undersaturated-oil-viscosity correlation (Dindoruk and Christman, 2004)

Coefficient (μ_{obp} correlation)	Value
a_1	0.776644115
a_2	0.987658646
a_3	-0.190564677
a_4	0.009147711
a_5	-0.000019111
a_6	0.0000063340

Using these correlations, we get the following graph:

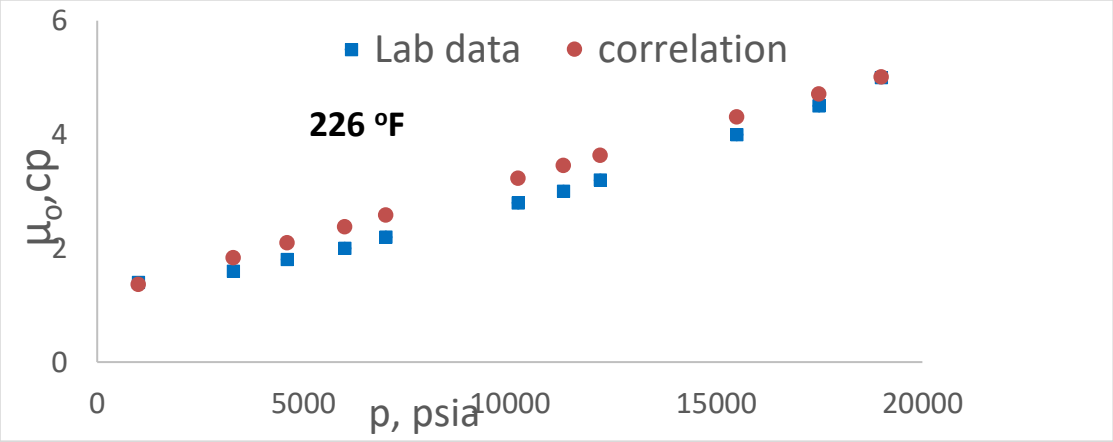

Fig. B.2: Comparison of proposed correlation with lab data

B.3 Oil Density

The oil being slightly compressible, its density varies along the flow path because of decrease in pressure and increase in temperature. We used a polynomial expression, Eq. B-1, to represent oil density, calibrated to represent the initial oil density used by App:

$$\rho = \rho_{o1} + (\rho_{o2}T + \rho_{o3})p^2 + 10^{-6}(\rho_{o4} + \rho_{o5}T)p - \rho_{o6}T \quad \text{(B.8)}$$

The following parameter values were used for oil density:

ρ_{o1}	ρ_{o2}	ρ_{o3}	ρ_{o4}	ρ_{o5}	P_{o6}
51	6.11E-12	-7.49E-09	412.031	0.5743	0.02372

An expression for J-T coefficient can be developed (Hasan et al. 2009) by considering the enthalpy of oil to be a function of pressure and temperature as follows:

$$\mathrm{d}H = \left(\frac{\partial H}{\partial T}\right)_p \mathrm{d}T + \left(\frac{\partial H}{\partial p}\right)_T \mathrm{d}p = c_P \mathrm{d}T - c_p C_J \mathrm{d}p \quad \text{(B.9)}$$

where

$$\left(\frac{\partial H}{\partial T}\right)_p = c_p \; and \; C_J \equiv \left(\frac{\partial T}{\partial p}\right)_H = \left(\frac{\partial T}{\partial H}\right)_p * \left(\frac{\partial H}{\partial p}\right)_T = -\frac{1}{c_p}\left(\frac{\partial H}{\partial p}\right)_T$$

So that, $c_p C_J = -\left(\frac{\partial H}{\partial p}\right)_T$ (B.10)

Eq. B-3 can be can be expressed in terms of fluid specific volume ($V \equiv 1/\rho$, lbm/ft^3) and its change with respect to temperature using Maxwell equations as follows:

$$\left(\frac{\partial H}{\partial p}\right)_T = V + T\left(\frac{\partial s}{\partial p}\right)_T \text{ and } \left(\frac{\partial s}{\partial p}\right)_T = -\left(\frac{\partial V}{\partial T}\right)_p$$

$$dH = c_p dT + \left[V - T\left(\frac{\partial V}{\partial T}\right)_p\right]\mathrm{d}p \quad \text{(B.11)}$$

We note that oil volume expansivity β is expressed as

$$\beta = \left(\frac{1}{V}\right)\left(\frac{\partial V}{\partial T}\right)_p \equiv \frac{1}{\rho}\left(\frac{\partial \rho}{\partial T}\right)_p \quad \text{(B.12)}$$

Combining Eq. B.1 and Eq. B.4, we obtain the following expression for the Joule-Thompson coefficient:

$$c_p C_J = -V\,[1 - T\beta] \tag{B.12}$$

For a constant enthalpy processes, dT = -C_J dp. Oil specific volume increases slightly with T, so that its expansivity β is small, positive number of the order of 10^{-4}/°F. Therefore, for liquids under usual reservoir conditions, (1—$T\beta$) is positive, usually between 0.95 and 1. In other words, the value of C_J is negative for liquids. Stated differently, as oil moves from the reservoir toward the wellbore, its pressure decreases, causing the temperature to increase because dT = −C_J dp, and both C_J and dp are negative. Eq. B.5 can be used to calculate C_J using the expression for density, Eq. B.1 as follows:

$$\left(\frac{\partial \rho}{\partial T}\right)_p = \rho_{o2} p^2 + 10^{-6}\rho_{o3} p - \rho_{o6} \tag{B.13}$$

$$\left(\frac{\partial \rho}{\partial T}\right)_T = 2(\rho_{o2} T + \rho_{o3}) p + 10^{-6}(\rho_{o4} + \rho_{05} T) \tag{B.14}$$

From Eq. B.5, we have

$$c_p C_J = -V(1 - T\beta) = \left(-\frac{1}{\rho}\right)\left[1 + \left(\frac{T}{\rho}\right)\left(\frac{\partial \rho}{\partial T}\right)_p\right]$$

$$c_p C_J = \left(-\frac{1}{\rho}\right)\{1 + \frac{T}{\rho}(\rho_{o2} p^2 + 10^{-6}\rho_{o3} p - \rho_{o6}) \tag{B.15}$$

B.4 Solution Gas-Oil Ratio

The solution gas oil ratio, for liquid gravity $\gamma_l \leq 30^o$ API,

$$R_s = \frac{\gamma_{gs} p^{1.0937}}{27.64}(10^{11.1724}) \text{ (B.10)}$$

And for $\gamma_l \geq 30^o$ API,

$$R_s = \frac{\gamma_{gs} p^{1.187}}{56.06} (10^{10.393A}) \quad \text{(B.16)}$$

Where $A = \frac{\gamma_l}{T+460}$ (B.17)

Here γ_l is liquid gravity, γ_{gs} is gas gravity in separator pressure.

B.5 Oil Formation Volume Factor

For pressure above bubble point, oil formation volume factor is

$$B_o = B_{ob} e^{c_o (p_b - p)} \quad \text{(B.18)}$$

Where $c_o = \frac{-1.433 + 5R_s + 17.2T - 1.180\gamma_{gs} + 12.61\gamma_l}{p \times 10^5}$ (B.19)

B_{ob} is oil formation volume factor at bubble point.

APPENDIX C

GAS PROPERTIES

C.1 Computational Procedure for Gases

From Hasan et al (2009):

$$c_p C_J = -[V - V - \left(\frac{VT}{Z}\right)\left(\frac{\partial Z}{\partial T}\right)_p = \left(\frac{VT}{Z}\right)\left(\frac{\partial Z}{\partial T}\right)_p \quad \text{(C.1)}$$

Eq. C.1 required accurate estimate of Z and $\left(\frac{\partial Z}{\partial T}\right)_p$. We use the following expression for these by Dranchuk et al (1973):

$$Z = 0.27p_r/T_r\rho \quad \text{(C.2)}$$

In Eq. C.2, ρ is a polynomial function of p_r (=p/pc) and T_r (=T/Tc)

$$f(\rho) = a\rho^6 + b\rho^3 + c\rho^2 + d\rho + e\rho^3(1 + f\rho^2)e^{-f\rho^2} - g \quad \text{(C.3)}$$

The constants are as follows:

a = 0.06423 b = $0.5353T_r$-0.6123

c = $0.3151T_r$ – 1.0467 -$0.5783/T_r^2$

d = T_r e = $0.6816/ T_r^2$ f = 0.6845 g = $0.27p_r$

From Eq. C.3, we get the derivative of ρ:

$$df(\rho) = 6a\rho^5 + 3b\rho^2 + 2c\rho + d + e\rho^2(3 + f\rho^2(3 - 2f\rho^2))e^{-f\rho^2} \quad \text{(C.4)}$$

$$\rho_{new} = \rho_{old} - \frac{f(\rho)}{df(\rho)} \quad \text{(C.5)}$$

The derivative of Z is obtained from Eq. C.2 as follows:

$$\left(\frac{\partial Z}{\partial T}\right)_p = 0.27p_r[\frac{\partial\left(\frac{1}{T_r}\right)}{\rho\partial T} + \frac{1}{T_r}\frac{\partial\left(\frac{1}{\rho}\right)}{\partial T} = .27p_r\left[\frac{1}{T_c T_r^2} + \frac{1}{T_r\rho^2}\frac{\partial\rho}{\partial T}\right] = \frac{0.27p_r}{T_r\rho}[\frac{1}{T} + \frac{1}{\rho}\frac{\partial\rho}{\partial T}] \quad \text{(C.6)}$$

From Eq. C.4, we get $\frac{\partial \rho}{\partial T}$

$$\frac{df(\rho)}{dT} = \left[6a\rho^5 + 3b\rho^2 + 2c\rho + d + e\rho^2\left(3 + f\rho^2(3 - 2f\rho^2)\right)e^{-f\rho^2}\right]\frac{\partial \rho}{\partial T} +$$

$$\frac{1}{T_c}\left[b_1\rho^3 + c_1\rho^2 + \frac{2c_3\rho^2}{T_r^3} + \rho - \frac{2e\rho^3}{T_r^3}(1 + f\rho^2)e^{-f\rho^2}\right] = 0 \qquad \text{(C.7)}$$

So, $\frac{\partial \rho}{\partial T} = -B/A$ (C.8)

Where, $A = \left[6a\rho^5 + 3b\rho^2 + 2c\rho + d + e\rho^2\left(3 + f\rho^2(3 - 2f\rho^2)\right)e^{-f\rho^2}\right]$

And $B = \frac{1}{T_c}\left[b_1\rho^3 + c_1\rho^2 + \frac{2c_3\rho^2}{T_r^3} + \rho - \frac{2e\rho^3}{T_r^3}(1 + f\rho^2)e^{-f\rho^2}\right]$